

# A Low-Frequency (30 – 110 MHz) Antenna System for Observations of Polarized Radio Emission from the Solar Corona

R. Ramesh · C. Kathiravan · M.S. SundaraRajan ·  
Indrajit V. Barve · C.V. Sastry

Received: 23 January 2008 / Accepted: 19 September 2008 / Published online: 14 October 2008  
© Springer Science+Business Media B.V. 2008

**Abstract** An interferometer antenna system to observe polarized radio emission from the solar corona at different frequencies in the range 30–110 MHz has been commissioned recently by the Indian Institute of Astrophysics at the Gauribidanur Radio Observatory (latitude  $13^{\circ}36'12''\text{N}$  and longitude  $77^{\circ}27'07''\text{E}$ ), about 100 km north of Bangalore ([http://www.iiap.res.in/centres\\_radio.htm](http://www.iiap.res.in/centres_radio.htm)). This paper describes the antenna system, associated analog/digital receiver setup, calibration scheme, and preliminary results.

**Keywords** Magnetic fields · Solar corona · Radio observations · Polarization

## 1. Introduction

The dynamics, structure, and evolution of the solar corona are controlled by its magnetic field. But a making a direct measurement of the latter in the low-density coronal plasma by means of the Zeeman or the Hanle effect is difficult (see Lin, Penn, and Tomczyk, 2000, and references therein). Since radio waves at frequencies  $< 150$  MHz from the Sun originate primarily in its corona, observations of polarized solar radio emission can be used to derive information about the magnetic field in the corona (Dulk and McLean, 1978). To determine the complete polarization state of an electromagnetic signal, it is necessary to measure all four Stokes parameters, that is: the  $I$ ,  $Q$ ,  $U$ , and  $V$ . Here  $I$  is the total intensity of the incident radiation.  $Q$  and  $U$  together specify the magnitude and orientation of the linear polarization, and  $V$  is a measure of the sense and intensity of the circular polarization. The usual practice in solar radio astronomy (particularly in this frequency range) is to employ a pair of mutually orthogonal linearly polarized antennae in conjunction with a phase switch to obtain different polarization parameters (see Cohen, 1958a, and Nelson, Sheridan, and

---

R. Ramesh (✉) · C. Kathiravan · M.S. SundaraRajan · I.V. Barve  
Indian Institute of Astrophysics, Koramangala, Bangalore 560 034, India  
e-mail: [ramesh@iiap.res.in](mailto:ramesh@iiap.res.in)

C.V. Sastry  
MEENAKSHI, No. 3, 2nd Cross, 1st Block, Koramangala, Bangalore 560 034, India

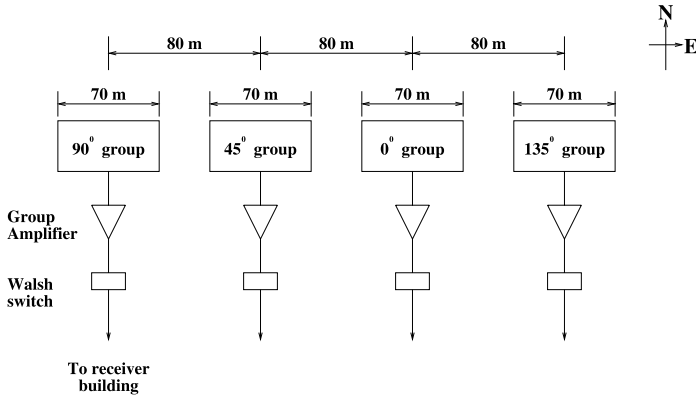


**Figure 1** Layout of the array.

Suzuki, 1985, for details on various solar radio polarization measurement techniques). In this paper, we describe an antenna system based on interference polarimetry (Morris, Radhakrishnan, and Seielstad, 1964) for dedicated observations of circularly polarized radio emission from the solar corona in the frequency range 30–110 MHz. Note that  $Q$  and  $U$  will generally be zero in our frequency range since Faraday rotation of the plane of linear polarization (both in the solar corona as well as the Earth's ionosphere) is considered to cancel the latter when the emission is summed over the observing band (Hatanaka, 1956; Grogard and McLean, 1973).

## 2. Array Configuration

The basic element used in the array is a log-periodic dipole (LPD). It is designed to operate in the frequency range 30–110 MHz with  $VSWR \leq 2$ , effective collecting area ( $A_e$ )  $\approx 0.5\lambda^2$ , characteristic impedance ( $Z_o$ )  $\approx 50 \Omega$ , and a directional gain  $\approx 8$  dB. The measured half-power beam widths are about  $60^\circ$  in the  $E$ -plane (parallel to the arms of the dipole) and  $100^\circ$  in the  $H$ -plane (perpendicular to the arms of the dipole). This enables us to carry out observations over a large range of hour angle and declination, respectively (see Ramesh, 1998, for more details on the LPD used in the array). The antenna system is a one-dimensional linear array of 32 LPDs in the East–West direction with a spacing of ten meters between adjacent LPDs. They are arranged as four groups with eight consecutive LPDs in each group. The length of each group is 70 meters and the spacing between phase centers of the adjacent groups is 80 meters. The arms of the LPDs in each group are oriented in a specific direction. Following the convention that is usually practiced in polarization work (Weiler, 1973), we considered terrestrial North as the reference and designated the group that has LPDs oriented in that direction to represent the  $0^\circ$  position angle (PA). The LPDs in the other three groups are oriented at  $PA = 45^\circ$ ,  $90^\circ$ , and  $135^\circ$  (measured in a counter-clockwise direction through the East) with respect to the reference (Figures 1 and 2). The total effective collecting area of each group is  $\approx 4\lambda^2$  (where  $\lambda$  is the wavelength of observation) and the minimum detectable flux density is about 200 Jy ( $1\text{Jy} = 10^{-22} \text{W m}^{-2} \text{Hz}^{-1}$ ) for one-second integration time. The total possible observation duration is  $\pm$  two hours around the local meridian ( $\approx 06:30$  UT).

**Figure 2** View of a section of the array. The orientation of the first LPD (near side) is  $135^\circ$  and that of the second LPD is  $0^\circ$ .



### 3. Group Configuration

The RF signal from each LPD in a group is passed through a high-pass filter that has a cutoff at 25 MHz and is then amplified by  $\approx 28$  dB in a wide-band amplifier. This pre-amplifier has a noise figure of  $\approx 3$  dB (300 K) and a bandpass extending from 0.5 to 500 MHz. The high-pass filter is used to cut off large interfering signals at frequencies  $< 25$  MHz, which otherwise can give rise to intermodulation products. In addition it also reduces the dynamic range requirements on the subsequent stages of electronics. The signals from the eight LPDs in a group are then combined in a eight-way power combiner. The output from the latter is amplified by  $\approx 34$  dB in a wide-band amplifier (group amplifier) and passed through an electronic switch that periodically inverts the phase of the input under the control of the Walsh switching signal transmitted from the central receiver building. The switched RF output from each group is passed on to the receiver room via coaxial cable buried about one meter beneath the ground level. The attenuation in the cable is  $\approx 2$  dB/100 meters at 100 MHz (Figure 3).

### 4. Analog Receiver

The RF signal from each antenna group is processed separately in the receiver building. To begin with, the signals are high-pass filtered to further suppress the spurious and interference signal at frequencies  $< 25$  MHz. The filter output is amplified by  $\approx 28$  dB and then up-converted to 170 MHz (intermediate frequency,  $IF_1$ ) by mixing with signal from a local

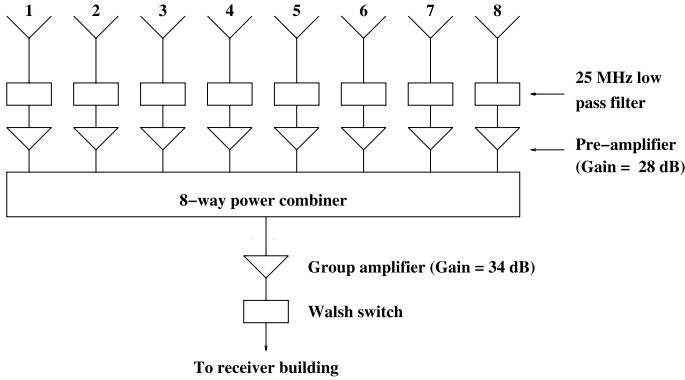


**Figure 3** Configuration of one of the groups in the array.

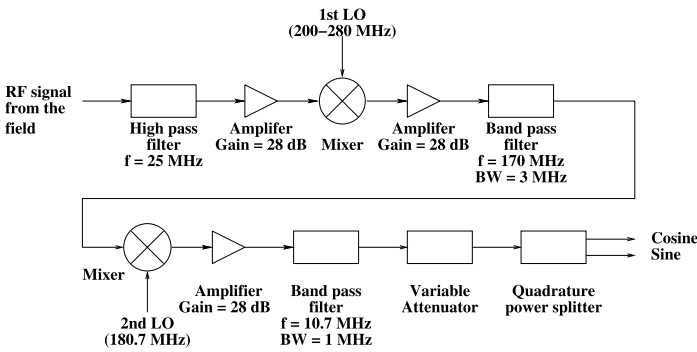


**Figure 4** Block diagram of the analog receiver.

oscillator ( $LO_1$ ), tunable to any particular spot frequency in the range 200–280 MHz. This conversion places the image frequencies well above the observing band (*i.e.*, 30–110 MHz). The insertion loss (IL) in the mixer used for this purpose is  $\approx 4$  dB. Multifrequency operation is achieved by sequentially tuning  $LO_1$  to the appropriate frequencies in the 200–280 MHz band. The output from the mixer is amplified by  $\approx 28$  dB and passed through a bandpass filter (IL  $\approx 6$  dB) with a center frequency ( $f_c$ ) of 170 MHz and a bandwidth (BW) of 3 MHz to suppress the signal at other frequencies. The signal is then down-converted to 10.7 MHz ( $IF_2$ ) by mixing with a second local oscillator signal ( $LO_2$ ) at a fixed frequency of 180.7 MHz. The output is again amplified by  $\approx 28$  dB and passed through a bandpass filter with  $f_c \approx 10.7$  MHz and BW  $\approx 1$  MHz to cut off contributions from unwanted signal at other frequencies. The combined insertion loss in this mixing and filtering operation is  $\approx 10$  dB, as in the earlier case. A variable attenuator (IL  $\approx 3$  dB) is placed at the output of the filter to adjust the input level to the correlator ( $V_{pp} \approx 100$  mV). The IF signal from each antenna group is then split into in-phase (cosine) and quadrature (sine) components by using an analog quadrature hybrid and finally fed to the digital correlator. Figure 4 shows the block diagram of the analog receiver.

## 5. Digital Receiver

To obtain all possible multiplications between the four antenna groups, a 12-channel digital correlator is used. The correlator system was built by using chips originally designed for the Nobeyama radioheliograph (Nakajima *et al.*, 1994) and the Gauribidanur radioheliograph (GRH, Ramesh *et al.*, 1998). These are custom-built chips that use CMOS gate array technology and they perform one-bit, two-level correlation. The correlator accepts inputs from four antennas and provides four complex correlations, corresponding to  $(2 \times 2)$  antenna pairs. Each cosine correlator gives output according to  $\overline{C_1 \oplus C_2} + \overline{S_1 \oplus S_2}$  and sine correlator according to  $\overline{C_1 \oplus S_2} - \overline{C_2 \oplus S_1}$ .

In the present setup, the 10.7-MHz IF signals are first quantized to two levels by using a zero-crossing detector. Then they are sampled at a rate of 2.04 MHz to avoid aliasing effects (Brigham, 1988). The basic element here is a high-speed comparator (AD 790). The latter gives “TTL” output depending on whether the input IF signal is above or below the “ground” level. The signal is then sampled in a D-type flip-flop (74LS74). An Ex-OR gate (74LS86) is used to demodulate the sampled signal for the phase inversion described in Section 3 (see Ramesh, 1998, and Ramesh, SundaraRajan, and Sastry, 2006, for details on this scheme). The sampled signal is then fed to the correlator. At the end of each integration period ( $\approx 256$  ms), the correlator output is written to a memory unit. The process of reading correlated data from each chip and writing into the memory unit goes on for 256 integration cycles. During this time, data that were written into another memory unit during the earlier 256 integration cycles are read into a computer. At the end of every 256 integration cycles, the role of the memory units gets reversed.

## 6. Calibration

One of the major problems in the study of polarized radio emission from the Sun and other sidereal sources is knowledge of the instrumental errors and appropriate procedures to minimize them. These include *i*) cross-talk between the antennas, *ii*) spurious effects from a combination of the direct radiation from the source and its reflection from the ground, and *iii*) off-axis effects (Morris, Radhakrishnan, and Seielstad, 1964). Antenna systems used for observations of polarized radio emission from the Sun in the past (particularly in the frequency range  $\leq 100$  MHz) were usually checked for their performance by feeding calibrated noise through a dipole mounted either onto a nearby high-rise structure or onto the antennas themselves (Cohen, 1958b; Suzuki and Tsuchiya, 1958; Bhonsle and McNarry, 1964). But since the collecting area is comparatively larger in the present case, we make use of observations of unpolarized sidereal sources at different declinations in the interval  $+23^\circ$  N to  $-23^\circ$  S (the latitude range over which the Sun moves in a year) to estimate the instrumental errors. This implies that the errors in circular polarization measurement on the Sun can be effectively removed by choosing an appropriate calibrator in and around the same region of the sky. Figures 5 and 6 show the total and circularly polarized intensity observations of Cygnus A, one of the intense calibrators in our frequency range (with flux density  $\approx 16500$  Jy at 77 MHz). It is clear from Figure 6 that spurious circular polarization from cross-talk, ground reflection, and off-axis effects is minimal and can be neglected. We have specifically used observations of Cygnus A for illustration here since it is a high declination source ( $\delta \approx 41^\circ$  N) for our array. The zenith angle of the source at its meridian transit is  $\approx 27^\circ$ . So any error in the measurement of circular polarization caused by ground reflection and/or off-axis effects is expected to be more pronounced in this case (Morris, Radhakrishnan, and Seielstad, 1964).

**Figure 5** Time profile of the total intensity  $I$  from Cygnus A observed on 24 March 2006 at 77 MHz during its meridian transit. The sample interval is 256 ms. The observations were carried out in transit mode and the plot is the “square” of the response (“voltage”) pattern of the antenna groups involved.

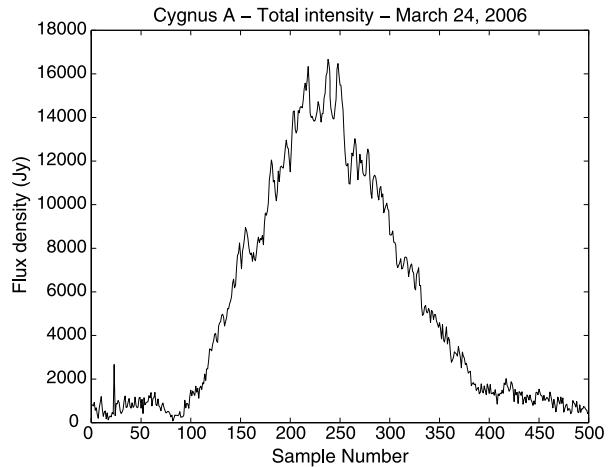
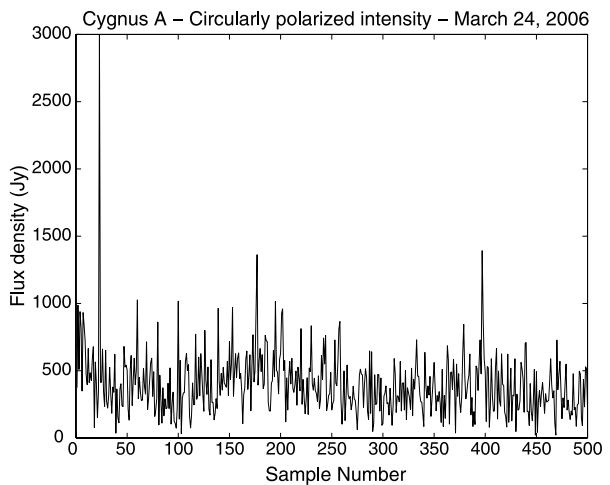


**Figure 6** Time profile of the circularly polarized intensity from Cygnus A observed on 24 March 2006 over the baseline between antenna groups  $0^\circ$  and  $90^\circ$ . One can notice that the instrumental circular polarization is minimal.



We carry out multiplications between all the antenna groups in the array and obtain six complex visibilities ( $S_{ij}$ , where  $i$  and  $j$  represent the orientation of the LPDs in the respective group) every 256 ms. They are  $S_{0,45}$ ,  $S_{0,90}$ ,  $S_{0,135}$ ,  $S_{45,90}$ ,  $S_{45,135}$ , and  $S_{90,135}$ . Since the length of the array is too small to resolve the Sun and other sidereal sources, we deal only with the amplitude of the observed complex visibility on each baseline. As a result, only the average polarization characteristics of the source are obtained (Ramesh and Sastry, 2005). The amplitudes corresponding to the visibilities  $S_{0,45}$ ,  $S_{0,135}$ ,  $S_{45,90}$ , and  $S_{90,135}$  are added and divided by four to estimate the total intensity  $I$ , as described in Weiler (1973). Observations of unpolarized sources with known flux density are used to estimate the total intensity  $I$  from the Sun in this case.  $S_{0,90}$  and  $S_{45,135}$  will be nonzero only if the incident radiation is circularly polarized. So any output (above the noise level) obtained in these two channels while observing an unpolarized calibrator can be attributed to instrumental errors. Calibrating the output against the corresponding total intensity  $I$  from the source provides a quantitative estimate of the amplitude of the error in terms of the latter. We are justified in adopting this scheme in our case since the complex gain of each antenna group and its associated receiver

**Figure 7** Time profile of the total intensity  $I$  from the Sun observed on 24 March 2006 at 77 MHz during its meridian transit.

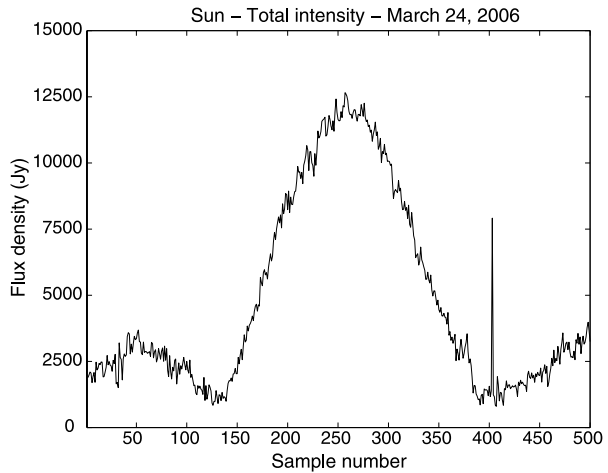
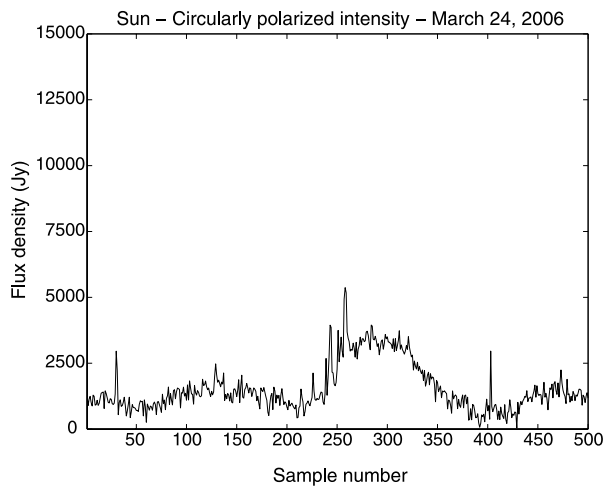


**Figure 8** Time profile of the circularly polarized intensity from the Sun observed on 24 March 2006 over the baseline between antenna groups  $0^\circ$  and  $90^\circ$ . The noticeable deflection above the noise level indicates the possible detection of circularly polarized radio emission from the solar corona at 77 MHz. The shift in the peak of the deflection as compared to Figure 7 is due to the phase error between the antenna groups involved.



chain are routinely checked and corrected for the differences among them by feeding a test signal. In this way we know the fraction of total intensity  $I$  (from the Sun) that should be subtracted from the amplitude corresponding to the visibilities  $S_{0,90}$  and  $S_{45,135}$  (again from the Sun) to get the “true” circularly polarized intensity. Note that there are not many polarized calibrator sources in our frequency range (Hanbury Brown, Palmer, and Thompson, 1955; Kraus, 1966) to carry out a direct calibration of these two visibilities.

## 7. Initial Results

Figures 7 and 8 show the solar observations carried out on 24 March 2006 around 06:30 UT at 77 MHz. No radio burst activity was noticed during our observing period with either the GRH or the solar radio spectrograph in our observatory (see Ebenezer *et al.*, 2007, for details on the latter). The solar data were calibrated as described in Section 6 by using observations of the sidereal source Virgo A carried out on the same day. The observed total flux density from the Sun was  $\approx 12400$  Jy (Figure 7). The corresponding output from the  $0^\circ$

**Figure 9** Radioheliogram obtained with the GRH at 115 MHz on 24 March 2006 around 06:30 UT. The open circle at the center is the solar limb. The instrument beam is shown near the bottom right corner. The peak brightness temperature is  $1.1 \times 10^6$  K and it corresponds to the discrete source close to the west limb.

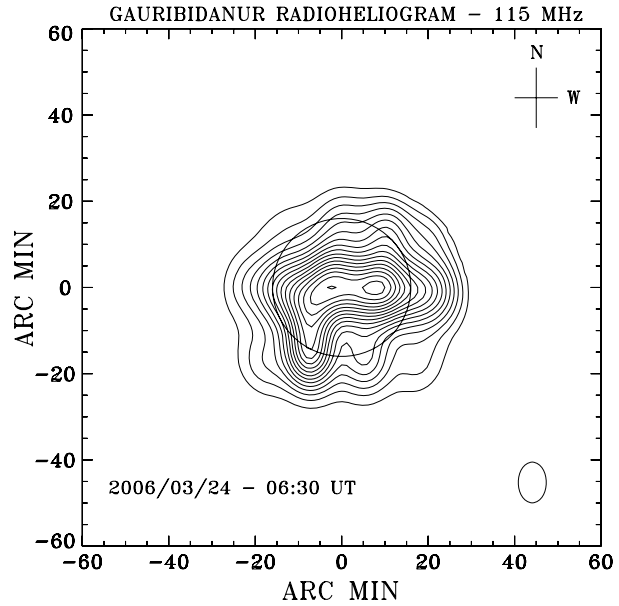
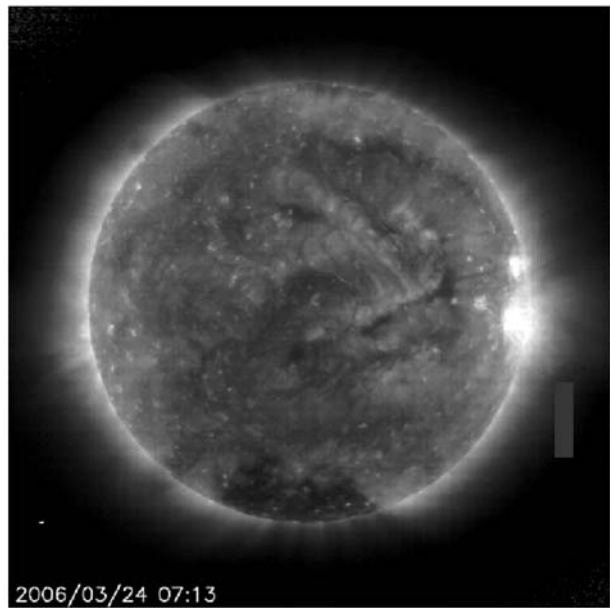


**Figure 10** 195 Å image of the solar corona obtained with the Extreme ultraviolet Imaging Telescope (EIT) onboard the *Solar and Heliospheric Observatory* (SOHO) on 24 March 2006 at 07:13 UT.



and  $90^\circ$  oriented antenna groups is shown in Figure 8. The presence of noticeable deflection above the noise level indicates the detection of circularly polarized radio emission from the solar corona at 77 MHz. The estimated flux density of the latter was  $\approx 2900$  Jy. The output from the  $45^\circ$  and  $135^\circ$  antenna groups also showed a similar deflection. We looked into the radioheliogram obtained with GRH at 115 MHz on that day (Figure 9) and the corresponding SOHO/EIT 195 Å image of the solar corona (Figure 10) to identify the source of the

observed circular polarization in the solar atmosphere. Except for the presence of a bright active region close to the west limb in both Figures 9 and 10, the Sun was “undisturbed.” No H $\alpha$ /X-ray flare or radio burst emission was reported (<http://sec.noaa.gov/>). Therefore it is possible that the observed polarized radio emission corresponds most likely to the aforementioned active region. A detailed report on this observation will be reported elsewhere.

## 8. Conclusions

An interferometer antenna system for observations of polarized radio emission from the Sun in the frequency range 30–110 MHz has been commissioned at the Gauribidanur Radio Observatory near Bangalore in India. Along with the existing radioheliograph and spectrograph at the observatory (which provide continuous data on the Sun for about six hours everyday), the polarization interferometer described in this paper is expected to play a useful role in the study of radio emission from the solar corona in the coming years.

**Acknowledgements** We thank C. Nanje Gowda, A. Anwar Saheb, G.S. Suryanarayana, and other staff members of the Gauribidanur Radio Observatory for their help in setting up the array and analog receiver system and in carrying out regular observations. D. Babu is thanked for his assistance in assembling and testing of the digital correlator receiver.

## References

- Bhonsle, R.V., McNarry, L.R.: 1964, *Can. J. Phys.* **42**, 292.
- Brigham, E.O.: 1988, *The Fast Fourier Transform and Its Applications*, Prentice-Hall, Englewood Cliffs, 322.
- Cohen, M.J.: 1958a, *Proc. Inst. Radio Eng.* **46**, 172.
- Cohen, M.J.: 1958b, *Proc. Inst. Radio Eng.* **46**, 183.
- Dulk, G.A., McLean, D.J.: 1978, *Solar Phys.* **57**, 279.
- Ebenezer, E., Subramanian, K.R., Ramesh, R., SundaraRajan, M.S., Kathiravan, C.: 2007, *Bull. Astron. Soc. India* **35**, 111.
- Grognard, R.J.-M., McLean, D.J.: 1973, *Solar Phys.* **29**, 149.
- Hanbury Brown, R., Palmer, H.P., Thompson, A.R.: 1955, *Mon. Not. Roy Astron. Soc.* **115**, 487.
- Hatanaka, T.: 1956, *Publ. Astron. Soc. Japan* **8**, 73.
- Lin, H., Penn, M.J., Tomczyk, S.: 2000, *Astrophys. J.* **541**, L83.
- Kraus, J.D.: 1966, *Radio Astronomy*, McGraw-Hill Inc., New York.
- Morris, D., Radhakrishnan, V., Seielstad, G.A.: 1964, *Astrophys. J.* **139**, 551.
- Nakajima, H., et al.: 1994, *Proc. Inst. Electr. Electron. Eng.* **82**, 705.
- Nelson, G.J., Sheridan, K.V., Suzuki, S.: 1985, In: McLean, D.J., Labrum, N.R. (eds.) *Solar Radio Physics*, Cambridge University Press, Cambridge, 113.
- Ramesh, R.: 1998, Ph.D. Thesis. <http://print.iiap.res.in/handle/2248/99>.
- Ramesh, R., Sastry, Ch.V.: 2005, In: Sankarasubramanian, K., Penn, M., Pevtsov, A. (eds.) *Large-Scale Structures and their Role in Solar Activity*, *Publ. Astron. Soc. Pac.* **346**, 153.
- Ramesh, R., SundaraRajan, M.S., Sastry, Ch.V.: 2006, *Exp. Astron.* **21**, 31.
- Ramesh, R., Subramanian, K.R., SundaraRajan, M.S., Sastry, Ch.V.: 1998, *Solar Phys.* **181**, 439.
- Suzuki, S., Tsuchiya, A.J.: 1958, *Proc. Inst. Radio Eng.* **46**, 190.
- Weiler, K.W.: 1973, *Astron. Astrophys.* **26**, 403.